A connection between magma chamber processes and eruptive styles revealed at Nisyros-Yali volcano (Greece)

Răzvan-Gabriel Popa[1*], Olivier Bachmann[1], Ben S. Ellis[1], Wim Degruyter[2], Peter Tollan[3], Konstantinos Kyriakopoulos[4]

[1]Institute of Geochemistry and Petrology, ETH Zürich, Clausiusstrasse 25, CH-8092 Zürich, Switzerland

[2]School of Earth and Ocean Sciences, Cardiff University, Main Building, Park Place, Cardiff, CF10 3AT, Wales, United Kingdom

[3] Institute of Geological Sciences, University of Bern, Baltzerstrasse 1-3, CH-3012 Bern, Switzerland

[4]Department of Geology and Geoenvironment, University of Athens, Panepistimiopolis, Gr-15784 Athens, Greece

ABSTRACT

Arc volcanoes generally emit water-rich, high-viscosity silicic magmas, which are prone to erupt explosively. However, effusive behavior is a common occurrence despite the high-H_2O, high viscosity conditions. The contrasting shift from effusive to explosive behavior (and vice-versa) at any individual volcano raises the question on what controls eruptive style. Permeability development in conduits allows magma to outgas and is clearly a key factor. However, an important question is whether magma reservoir processes can also have an influence on eruptive styles. The answer could have direct impact on predicting eruptive behavior. Hence, we explore this potential connection by analyzing nine alternating effusive and explosive silicic deposits that were emplaced during distinct eruptions at the active Nisyros-Yali volcanic center. The lavas and pyroclastic deposits are compositionally similar. This indicates a negligible influence of the bulk rock composition on different eruptive styles. The crystal contents vary between units, without any clear correlation with eruptive style (from nearly aphyric to ~45 vol% crystals). Mineral textures and chemistry do show variations between effusive and explosive eruptions, with a larger proportion of resorbed plagioclase and more evolved amphiboles present in the lava flows. Mineral thermo-barometry and hygrometry show that the storage zones of magmas generating effusive eruptions evolved towards colder and more water-rich conditions (710-790˚C; 5.6-6.5 wt% H_2O) than their explosive counterparts (815-850˚C; 4.2-4.6 wt% H_2O). At storage pressures of 1.5-2 kbar, relevant for Nisyros-Yali, the volatile saturation level is reached at > 5 wt% H_2O. It is likely that the magmas reached water-saturation before generating effusive eruptions, and were undersaturated before explosive events. We hypothesize that the presence of exsolved gas in the subvolcanic reservoir can enhance the outgassing potential of the magma during conduit ascent. Hence, the rhyolitic effusive-explosive transitions can be influenced by the pre-eruptive exsolved versus dissolved state of the volatiles in the magma chamber. This can lead to the less explosive eruptions for the most water-rich reservoir conditions.

THE EFFUSIVE-EXPLOSIVE TRANSITION.

Predicting the eruptive style of volcanoes and determining the extent to which it correlates to the physical state of the magma chamber is a major challenge of modern volcanology (National Academies of Sciences, 2017). Individual volcanoes of all magmatic compositions can erupt either effusively or explosively. The change from one style to the other can take place during the same eruption, or it can take place in separate, independent events (Cassidy et al., 2018). Either way, this phenomenon has implications for risk assessment because variations in eruptive style imply widely different volcanic hazards (Parfitt and Wilson, 2008).

The effusive-explosive transition is a generic term defining effusive-to-explosive, but also explosive-to-effusive changes. It is related to (i) surface events such as dome collapse or to (ii) changes in the style and degree of fragmentation during magma ascent. The fragmentation process can be influenced by magma-water interaction (hydromagmatic processes) (Morrissey et al., 2000), or it can be a purely magmatic feature. In the second scenario, fragmentation takes place in the conduit without any interaction with external factors (Gonnermann and Manga, 2013). Here, the absence of an independent trigger (*i.e*. water sources or sector collapse) makes the change in eruptive style challenging to predict.

Magmatic fragmentation tends to be more efficient when the eruptions are generated by rhyolitic magmas. This is due to the high volatile contents and high viscosities of the magmas, which combine to generate energetic explosive events (Dingwell, 1996; Papale, 1999). However, water-rich silicic magmas often generate effusive eruptions that do not show compositional changes with respect to their explosive counterparts (Eichelberger et al., 1986; Edmonds and Herd, 2007; Ruprecht and Bachmann, 2010). This means that changes in eruptive style can occur regardless of magmatic composition, making it harder still to anticipate.

In the case of magmatic fragmentation, conduit processes dictate the eruptive style. For example, Eichelberger et al. (1986) links the change in eruptive style of compositionally similar magmas to permeability development and outgassing in the shallow conduit. Subsequent studies support this (Woods and Koyaguchi, 1994; Klug and Cashmann, 1996; Edmonds and Herd., 2007; Degruyter et al., 2012; Castro et al., 2012). However, the mechanisms that allow permeability and outgassing to develop are complicated, and all the feedbacks are not yet fully understood. For example, viscous-shear at the conduit wall promotes outgassing: this lowers the explosive potential of the melt and leads to an effusive eruption (Gonnermann and Manga, 2003). Meanwhile, friction along the conduit wall lubricates the melt: this increases ascent rate and promotes explosivity (Pollaci et al., 2005). Ascent velocity has also been directly linked to eruptive style (Nguyen et al., 2014). However, complex feedbacks between ascent velocity, bubble growth and fragmentation (Parfitt and Wilson, 2008) makes it complicated to determine whether ascent rate is a cause or an effect of eruptive style. These few examples illustrate the complexity of conduit processes. Pre-ascent properties of the magmas, such as composition, temperature, crystallinity and volatile budgets complicate the picture even more.

The physical and chemical state of the magma chamber likely influences the conduit processes. In line with this, recent work suggests that changes in eruptive styles can be linked to reheating via primitive magma recharge (Ruprecht and Bachmann, 2010; Koleszar et al., 2012; Degruyter et al., 2017), to the presence of an exsolved volatile phase in the magma chamber (Degruyter et al., 2017), to volatile dilution (Cassidy et al., 2016) and to the structure of the silicate melts (Di Genova et al., 2017). The common hypothesis is that although the magmatic effusive-explosive transition occurs in the conduit, its cause might be rooted in the magma reservoir, before magma ascent is triggered. If this is accurate, it will open new possibilities to model and to enhance our forecast capabilities of eruption style based on volcano monitoring.

In this paper, we explore the potential effects of magma chamber processes on the magmatic effusive-explosive transition. This is done via petrological and geochemical investigations of the active Nisyros-Yali rhyolitic volcanic center, located in the South Aegean Arc (Fig. 1). Over the past 161 ky (Bachmann et al., 2012), the volcanic center erupted lavas of a wide compositional variability (Di Paola, 1974). The volcano evolved from a basaltic andesite seamount to a stratovolcanic island built by subsequent eruptions of andesitic to dacitic magmas (Di Paola, 1974; Francalanci et al., 1995). These compositionally intermediate magmas potentially originated from the lower crust (Klaver et al. 2018). Their extrusion culminated with the emplacement of the voluminous Emborios dacitic domes on the flanks of the stratovolcano (Dietrich and Lagios, 2017). In the following stage of activity, potentially in the last 100–110 ky (Rehren, 1988; Tomlinson et al., 2012; Guillong et al., 2014), Nisyros erupted only rhyolitic and rhyodacitic magmas originating from the upper-crustal silicic mush (Bachmann et al., 2012; Klaver et al., 2017; Bachmann et al., 2019). During this period, the eruption styles alternated between the extrusion of the massive Avlaki and Nikia lava flows and two subplinian events responsible for emplacing the Lower and Upper Pumice deposits (Longchamp et al., 2011) at N48 ka (Tomlinson et al., 2012). These explosive eruptions shaped the present-day caldera morphology of the island, which was later partly filled with rhyodacite domes ("post-caldera domes") (Seymour and Vlassopoulos, 1989; Braschi et al., 2012). After the last caldera-collapse on Nisyros (Upper Pumice event), volcanic activity also took place ~5 km to the NW (Allen and McPhie, 2000; Dietrich and Lagios, 2017). Here, over the past 45 ky (Guillong et al., 2016) two rhyolitic explosive events and one rhyolitic effusive eruption (an obsidian flow) created the smaller island of Yali. Nowadays, intense fumarolic activity takes place on the caldera floor of Nisyros and the volcano occasionally shows signs of unrest (Chiodini et al., 2002; Bini et al., 2019).

The Nisyros-Yali volcanic area offers a good opportunity to study nine individual silicic units (Fig. 2), five lava flows and four tephra deposits, which reflect the repeated magmatic transition between explosive and effusive behavior. Moreover, effusive and explosive deposits were emplaced during distinct eruptive events. This gives the opportunity to connect changes in eruptive styles to potential changes in the chemical and physical state of the magma chamber. We therefore present a large comparative petrological and geochemical dataset to address the issue of magmatic effusive-explosive transitions at this particular volcano.

METHODS.

Fresh, unaltered samples were collected from deposits of 9 successive eruptions that took place on the islands of Nisyros (6 eruptions) and Yali (3 eruptions) (Fig. 2). Where possible, the deposits were sampled at different locations, to assess any potential local heterogeneity. The exact sampling locations are given in table ST1 of the supplementary material. In the case of effusive deposits, we mostly sampled glassy outcrops that were subject to shorter cooling timescales. We sampled areas that were not visibly percolated by gas and that were not enclave-rich. We extracted the enclaves that were macroscopically visible, before any further sample preparation was done. For the post-caldera effusive volcanism, 8 individual domes were sampled and analyzed. In the case of the explosive events, we collected pumices from both pyroclastic fall and pyroclastic flow deposits. We chose only fresh pumices from non-welded deposits. We did not analyze the crystal-rich pumices that are, in any case, very rare. Also, we avoided sampling banded or streaky pumices, unless we aimed at extracting the enclaves.

In the following, an overview of the analytical methods used to investigate mineral, groundmass glass and bulk rock compositions is presented. The complete analytical details can be consulted in section A of the supplementary material and the complete dataset (amphibole, orthopyroxene, clinopyroxene, Fe-Ti oxide, groundmass glass, bulk-rock, plagioclase rims) can be found in tables ST2-ST8 of the data repository. Unless stated otherwise, all analyses were performed in the laboratories of ETH Zürich.

Minerals and groundmass glasses were analyzed by using a combination of electron probe micro-analysis (EPMA), calibrated scanning electron microscopy (SEM) and laser-ablation inductively-coupled plasma mass spectrometry (LA-ICPMS). The major element and selected trace element compositions of amphibole, pyroxene and Fe-Ti oxide were analyzed with a JEOL JXA-8200 Electron Probe Microanalyzer at 15 kV, 20 nA with a focused beam. For measuring the composition of groundmass glasses in microlite-poor samples, the Microanalyser was recalibrated and set at an acceleration voltage of 15kV, intensity of 0.5 nA and the beam defocused to 15 µm. The glasses were also analyzed with an EDS-calibrated JEOL JSM-6390 LA Scanning Electron Microscope with a Thermo Fisher NORAN NSS7 EDS system (LaB_6 filament, 30 mm^2 silicon-drift detector and Faraday-cup for calibration) that allows averaging measurements over wide areas (*e.g.* 50 µm diameter). This was useful for eliminating the late-stage differentiation effect of post-emplacement microlite crystallization in the microlite-rich effusive units. In this particular case, the fine-scaled EPMA cannot be used to estimate pre-eruptive melt compositions and any measurements would be biased by post-emplacement crystallization. When both analytical methods were used on the same microlite-free samples, EPMA and SEM yielded similar results that are compared in table ST6 (data repository). The SEM analyses are discussed in the paper since this dataset covers the whole range of effusive and explosive units. The same calibrated SEM was employed for analyzing the major elemental composition of plagioclase rims. Trace element analyses of minerals (amphiboles, pyroxenes) and groundmass glasses were performed with a Resonetics Resolution S155 laser ablation connected to a Thermo Element XR sector-field mass spectrometer. The samples were ablated for 30 s at spot sizes between 19 µm and 29 µm, at a repetition rate of 5 Hz and an energy of ~3.50 J/cm^2 (using NIST610 as primary standard and SiO_2 and CaO EPMA data as internal standards input in the SILLS software of Guillong et al., 2008). In order to obtain trace elemental analyses of groundmass

glass in microlite-rich lavas, the microlites were ablated together with the glass using large aperture laser spots, and the compositions automatically averaged, in a similar fashion to the SEM approach.

Whole-rock major and selected trace element analyses were performed on fused glass discs (rock powders dehumidified at 110 ˚C, devolatilized at 850˚C and fused at 1200˚C after mixing with a Lithium-Tetraborate flux) with a PANalytical AXIOS wave-length dispersive X-ray fluorescence spectrometer. The trace element analyses were later performed with a 193 nm ArF-Excimer (Geolas) laser connected to an Elan6100 DRC quadrupole ICP mass spectrometer. 40 μm spots were ablated for 30 seconds at a repetition rate of 10 Hz, using a similar approach as previously mentioned.

Crystallinity (porphyritic index) was determined by X-ray powder diffraction for pumices and by thin section point counting for lava samples (to avoid the effect of microlites). The XRD analyses were performed with an AXS D8 Advance spectrometer with a Lynxeye detector (40 kV and 40 mA current, 5-90˚ scans with 0.8 seconds step time). A calibration curve based on glasses containing known vol% crystals (Forni et al., 2016) was used to determine the porphyritic index (Rowe et al., 2012). Between 1 and 3 individual pieces of pumice were analyzed at the XRD for each explosive unit.

The glass structure and H_2O contents of melt inclusions were assessed qualitatively by Fourier transform infrared spectroscopy (FTIR) at the University of Bern, using a Bruker Tensor II spectrometer with a globar source and Bruker Hyperion 3000 microscope. Analyses were performed with an attenuated total reflectance (ATR) objective, coupled with a liquid nitrogen-cooled focal plane (FPA) array mapping detector. The ATR crystal is constructed from germanium (refractive index of 4.0) and has an angle of incidence of 45°. Spectra were acquired with a resolution of 8 cm^{-1} and 128 scans over a wavenumber range of 900-3850 cm^{-1}, with a background on air measured before every sample. Spectra were initially acquired at the full spatial resolution of the FPA detector (~0.5 μm), but the data were subsequently binned to achieve higher spectral quality, resulting in a final spatial resolution of ~4 μm. The data were processed using the OPUS software package. The spectra were corrected for the wavenumber-specific ATR absorbance using the "Extended ATR correction" tool, assuming a glass refractive index of 1.5 and a single ATR reflection.

RESULTS.

The geochemical record.

Effusive and explosive deposits at Nisyros-Yali are geochemically similar (Fig. 3A) and eruptive styles are not correlated with either bulk-rock or melt composition. For example, rhyodacites (~70 wt% SiO_2) and high silica rhyolites (77 wt% SiO_2) have generated both styles of eruption. The variability seen in the major elemental behavior of bulk-rocks and groundmass glasses (Fig. 3B-G) reflects the interplay between differentiation and recharge events. This interplay can induce slight differences between units. For example, the Post-Caldera domes and the Upper Yali Pumice are a little less evolved than the units that erupted before them (Fig. 3B-G). This is reflected in the trace elemental behavior of both bulk-rocks and groundmass glasses (Fig. 3H,I). Otherwise, the trace elements are consistent with the rest of the data and do not indicate any difference between magmas generating effusive and explosive events.

Magmatic enclaves of andesitic and basaltic andesite composition are present in effusive and explosive deposits, alike (Fig. 3A). The enclaves are that we analyzed are vesiculated, and have round and cauliform shapes, with sharp contacts with the host magmas. They likely represent fragments of mingled mafic recharge into the more silicic reservoirs.

The petrological record.

The mineralogy of the effusive and explosive units is similar. The rocks contain plagioclase, orthopyroxene, hornblende, Fe-Ti oxides and rare clinopyroxene, as well as small amounts of zircon and apatite. Biotite is observed in units 4 (Nikia flow) and younger, and quartz is found in units 6 and 9 (the Nisyros Post-caldera and Yali Obsidian effusive events). Overall, crystallinity varies significantly, but both eruptive styles were generated by magmas of low (<5% vol.) and high (>30% vol.) crystallinity, alike (Fig. 4). Explosive events are typically less crystal-rich, but the Upper Pumice has up to 30 vol% crystals (PI confirmed in 3 different pumice samples).

The compositional variability of pyroxenes suggests that two distinct populations are present in all deposits, irrespective of eruptive style (Fig. 5). (i) Unzoned orthopyroxenes and clinopyroxenes form narrow, well-defined compositional groups characterized by high-Mn and low-Mg#. With the exception of Emborios, they do not pass the melt equilibrium tests of Putirka (2008) and thus reflect earlier, relict or periodic stages of crystallization. We interpret these to be phenocrysts developed in the Nisyros-Yali mush system. In addition, (ii) less differentiated ortho- and clinopyroxenes of higher Mg# are ubiquitous throughout effusive and explosive deposits. When complexly zoned, these can be interpreted as antecrysts. However, many of the high Mg# pyroxenes have homogenous compositions, without grading to normally zoned rims. These are mafic recharge crystals, originating from deeper in the system. In addition, syn-eruptive orthopyroxene microlites are present in effusive units.

The plagioclase crystals ubiquitously record the effects of magma recharge, but show some differences between eruptive styles. In both effusive and explosive units, most of the plagioclase generally varies between 30-50 molar An%, with the addition of more calcic component, up to 80-90 molar An% (Dietrich and Popa, 2017) that suggests inheritance from deeper recharge. The low-An phenocrysts, specific for the Nisyros-Yali mush system, are normally zoned with occasional oscillations. Zoning patterns are accompanied by resorption and/or skeletal overgrowth textures rich in vesicles (former fluid inclusions). The fluid inclusions are observed only in effusive units (Fig. 6B, 6R). Additionally, based on the aspect of the crystal-glass interface, plagioclase crystals can be divided into a resorbed and un-resorbed (euhedral) population (Fig. 6A). In explosive deposits, the distribution of the two populations is rather balanced, whereas in the effusive units resorbed crystal dominate (75% - 100% of plagioclase). There are no systematic compositional differences between the resorbed and euhedral populations.

The amphiboles record the most profound compositional difference between effusive and explosive deposits, both in major and trace elements (Fig. 7). In the explosive units, they show little compositional variability, with relatively high Al_{IV}-Ti concentrations (1.4-2 apfu and 0.2-0.4 apfu, respectively). In contrast, the amphiboles found in lavas record a wider compositional range that grades down to low Al_{IV}-Ti values (0.8 apfu and <0.05 apfu, respectively). The Lower Yali Pumice is the only explosive deposit to exhibit two distinct amphibole populations. These are compositionally homogenous crystals, located towards

both ends of the Nisyros-Yali compositional spectrum. However, the low Al_{IV}-Ti amphiboles represent less than 30% of the Lower Yali amphiboles and are likely relicts from more evolved portions of the mush. Additionally, throughout the units there is a good correlation between Al_{IV} and Ti on one side (Fig. 7A), and the trace element distribution on the other (Fig. 7B). For example, a decrease in Al_{IV} –Ti is marked by a decrease in the concentration of compatible trace elements (*i.e.* Sr) and by an increase in incompatibles (*i.e.* Ce). The compositional difference between the „effusive" and „explosive" amphiboles is consistent with the zoning patterns of the crystals (Supplementary Fig. S1). In explosive deposits the amphiboles are relatively unzoned, which accounts for the thermo-chemical stability of the system. In the effusive deposits the crystals are generally normally zoned, with decreasing Al_{IV}-Ti towards the rims. In lava flows, there are also homogenous, low Al_{IV}-Ti amphiboles. There are, however, two noticeable exceptions from these trends:

1. The Lower Yali Pumice is the only explosive deposit to exhibit two distinct amphibole populations. These are compositionally homoge- nous crystals, located towards both ends of the Nisyros-Yali compo- sitional spectrum. There is no compositional grading between the two. However, the low Al_{IV}-Ti amphiboles represent b30% of the Lower Yali amphiboles and are likely relicts from more evolved por- tions of the upper-crustal silicic mush. The high Al_{IV}-Ti amphiboles, which are similar to those found in the other explosive deposits, are dominant and seemingly in equilibrium with the other phases of the Lower Yali.
2. The Post-caldera domes have higher Al amphiboles, around 1.7–2.1 apfu Al_{IV}-Ti. These are generally small crystals, sometimes affected by resorption. Similar to the amphiboles present in the other lavas, they show dehydroxylation textures.

Fe-Ti oxides, magnetites and ilmenites, are pristine, unzoned, and compositionally homogenous irrespective of crystal size. The oxides do not generally exhibit exsolution lamellae. The exceptions are crystals found in slowly-cooled parts of the domes, where they have undergone post-eruption resetting. Such crystals are easily avoided by analyzing only glassy samples (most rapidly quenched). Fe-Ti oxides are ubiquitous throughout the Nisyros units, but ilmenites become scarce in the Yali deposits. Nonetheless, wherever found together, Mg-Mn equilibrium tests (Bacon and Hirschmann, 1988) suggest that magnetites and ilmenites co-crystallized (Supplementary Fig. S2). Disequilibrium crystals generally accounted for less than 5% of the dataset and were discarded. This provides a powerful tool for estimating eruptive magma temperatures.

DISCUSSION.

Differentiation, recharge and eruption triggering.

As is typical for stratovolcanoes with polybaric plumbing systems all over the world (Bachmann and Huber, 2016; Cashman et al., 2017), differentiation and magma recharge are the main reservoir processes that control the textural and compositional parameters of the Nisyros-Yali deposits. Differentiation dominates during the cooling periods, as indicated by the chemical evolution of the interstitial melts (e.g. Fig. 3 E-G, units 1-to-5). Recharge events occur from time to time, as clearly recorded by melt chemistry (e.g. Fig 3 E-G, units 5-6 and 7-8; Fig. 3I). In particular, there are many indicators that recharge events occur shortly prior to both effusive and explosive eruptions, and are likely the eruption-triggering factors:

1) the presence of the mafic, vesiculated enclaves described above. The preservation of these hot, gas-rich enclaves, as opposed to their disaggregation and chemical assimilation (e.g. Gill, 2010; Spera et al., 2016), is an indicator that the eruptions were triggered during or soon after the recharge event took place;
2) unzoned, high Mg# pyroxenes. These crystals indicate mafic origin. The absence of normally zoned overgrowths indicates that the crystals were extruded before normally zoned regrowth could take place, following the recharge event.
3) ubiquitous plagioclase resorption textures, without new overgrowths. Complete thermal re-equilibration following the recharge and heating event is not recorded in these crystals. It suggests a limited amount of time between the reheating event that triggered the resorption and the eruption.

A key geochemical observation in the Nisyros-Yali units is the contrasting elemental behavior of groundmass glasses (enclave-free) and bulk-rocks (including micro-enclaves). The groundmass glasses are typically more evolved and do not show much evidence for recharge, while the bulk-rocks clearly display it. Additionally, there are no crystals or overgrowths with intermediate compositions between the mush and recharge end-members, to suggest chemical hybridization. Therefore, recharge seems to have mostly generated magma mingling rather than chemical mixing, as is expected for magmas with highly different compositions and viscosities (Oldernburg et al., 1989; Lee and Bachmann, 2014). This is best illustrated for the highly differentiated Lower Yali and Yali Obsidian events, where the compositional effect of the recharge is minimal in both glasses and bulk-rocks (mingling is inhibited on the micro-scale and large enclaves are easily extracted during sample preparation). Hence, the recharge events do not significantly affect the interstitial melts, which provide a reliable record of melt compositions prior to the eruption-triggering recharges.

This is more difficult to evaluate for the Post-caldera domes and the Upper Yali pumice: both units record mafic signatures that tend to limit the effects of differentiation. However, the trace element data of orthopyroxenes and amphiboles shows that minerals are also consistently depleted in REEs and enriched in compatibles (e.g. Sr) compared to the other units (Supplementary Fig. S3; Fig. 8). This indicates that the phenocrysts found in these two units crystallized from less evolved melts, which were already prevalent before the eruption-triggering recharge occurred. These less evolved conditions are potentially induced by the evacuation caused by the last caldera collapse of Nisyros and by the first Yali explosive eruption (e.g. Braschi et al., 2012), which created space for recharge to be accommodated in the mush without eruptions being triggered. We argue that the groundmass glasses of all investigated units record the pre-eruptive, pre-recharge compositions of the melts, relevant for the storage conditions at the time of the eruption triggering event. This is in agreement with other independent evaluations that were performed on some of the units (Braschi et al., 2012; Klaver et al., 2018).

Interpretative choices and tools for reconstructing the pre-eruptive reservoir conditions.

A key difference between effusive and explosive deposits is the degree of differentiation reached by magmas before erupting. This is particularly well illustrated by the higher concentration of incompatible trace elements that is found in amphiboles from lava flows (Fig. 7). The data suggest that effusive eruptions were triggered after longer periods of

differentiation than their explosive counterparts record. The amphibole compositional variability also suggests that the effusive magmas reached colder conditions before erupting. These observations are evident for the Avlaki, Nikia and Yali Obsidian rhyolitic flows, while they do not apply for the older and less evolved Emborios dome. This is difficult to assess for the Post-caldera domes which are affected by inverse differentiation (they become slightly more primitive, as discussed above and in Braschi et al., 2012). Here, the amphiboles crystallized from a slightly more mafic composition and any direct comparison to those found in rhyolites is biased by the different chemical conditions. On the other hand, magmas generating explosive events always record generally warmer and more stable conditions (less chemical variation in minerals).

Overall, colder and more differentiated magmas preferentially generate effusive eruptions at Nisyros-Yali. This observation is unexpected, because it implies higher volatile contents and potentially higher viscosities that are typically believed to enhance the explosivity of the magma. To explore this further, we need to constrain the following: (i) the thermal conditions of the erupting magmas, (ii) the volatile contents, (iii) the melt viscosities at the time of extrusion and (iv) the storage pressures. Here, we will present the concepts, tools and interpretative choices we made to estimate these conditions. We pres- ent the results in the next section.

(i) The amount of pre-eruptive reheating plays a key role in the effusive-explosive transition, by influencing the eruptive temperature and the viscosity of the magma, as suggested for Volcan Quizapu (Ruprecht and Bachmann, 2010) and Mt Hood (Koleszar et al., 2012). The pre-eruptive reheating can be obtained by comparing post-recharge (eruptive) and pre-recharge (storage) temperatures (see Ruprecht and Bachmann, 2010). For example, eruptive temperatures are estimated through Fe-Ti oxide thermometry (Ghiorso and Evans, 2008). This is valid because Fe-Ti oxides equilibrate rapidly to the changing thermal conditions induced by the recharge event (Venezky and Rutherford, 1999). On the other hand, amphibole-plagioclase thermometry (Anderson and Smith, 1995; Holland and Blundy, 1994) can record the pre-recharge conditions, because re-equilibration time is slow for both minerals. To evaluate the temperatures immediately prior to the recharge event, we couple the normally zoned plagioclase rims with amphibole rims that are unaffected by breakdown. For units with multiple amphibole populations, the REE-rich, Al_{IV}-Ti poor crystals were used. This is not the case for the Lower Yali pumice, because the rarer low Al amphiboles seem to have evolved separately, without showing any compositional grading between them and the dominant amphi- bole population of this magma. They are likely relicts/antecrysts and are not reliable for thermometry calculations. Overall, the amphibole-plagioclase method is suitable for the case of Nisyros-Yali because:

- The Al record of amphiboles is unaffected by hydrogen diffusion during reheating, unless breakdown occurs (Graham et al., 1984);
- During conduit ascent, anhydrous assemblages of plagioclase, orthopyroxene and Fe-Ti oxides are stabilized as microlites, while amphibole growth is inhibited. This occurs because amphibole is destabilized during ascent by decompression and water loss (e.g. Rutherford and Hill, 1993; Browne and Gardner, 2006). Hence, syn-eruptive amphibole overgrowth is not expected;

- In plagioclase populations, the resorption textures are not sealed by overgrowths. Therefore, overgrowth of plagioclase does not occur during conduit ascent. Late stage crystallization is limited to the growth of microlites;
- Plagioclase rim compositions can still be recovered by measuring the euhedral population and the remnants of the partly resorbed rims.

The only caveat seems to be related to the Post-caldera domes, where amphibole-plagioclase equilibrium is harder to assess. This is mostly because of the Al-richer compositions of the amphiboles. They are different when compared to the other units and, as other authors observed, similar to enclave amphiboles (Klaver et al., 2017). However, as already discussed earlier in this paper, the Post-caldera domes also record a slightly different magmatic environment than the other units. The environment was characterized by a less evolved melt that determined minerals to record less evolved conditions: orthopyroxenes and clinopyroxenes depleted in REE and plagioclase rims that are more anorthitic compared to other units (closer to 40 An%, than 30 An%). Under these conditions, the amphiboles are expected to be more "mafic" than those found, for example, in the pumice deposits. Hence, we favor the interpretation of the amphiboles from the Post-caldera domes crystallizing in the upper-crustal silicic mush, as a result of an older melt hybridization event that changed the composition of the magmatic system. The storage temperatures of ~780 °C that we obtain from amphibole-plagioclase pairs for the Post-caldera domes (details in the next section) are in agreement with the presence of quartz and accessory biotite, which require storage temperatures of <800 °C (e.g. Rutherford and Devine, 2003; Marxer and Ulmer, 2019).

(ii) The volatile content of magmas (both dissolved in the melt, and exsolved as a fluid/gas phase) is clearly critical in influencing eruptive styles (e.g. Gardner 2009; Gonnermann and Manga, 2013). The dissolved volatile concentration in undersaturated melts is known to increase during magmatic differentiation, as H_2O behaves incompatibly. A direct measurement of water content is difficult to achieve at Nisyros-Yali because melt inclusions are generally scarce or crystallized in effusive units. This scarcity is probably linked to the lower storage temperatures of magmas generating effusive eruptions. The low temperatures lead to slower crystal growth rates that inhibit melt entrapment (e.g. Baker, 2008). Additionally, effusive deposits are subject to long post-emplacement cooling times. This means that, depending on the rate and mechanisms of H diffusion in the host crystals, melt inclusions from lava flows will suffer diffusive loss of H_2O (e.g. Bucholz et al., 2013; Gaetani et al., 2012). The reliability of the melt inclusions volatile record may be impacted further by cooling-induced CO_2 shrinkage bubbles (Wallace et al., 2015) and post-entrapment crystallization (e.g. Steele-Macinnis et al., 2011). Because of these caveats, direct measurements of water in effusive units will not yield accurate results (see Fig. 8 for Nisyros-Yali).

More reliable for such units is the plagioclase-melt hygrometer (Waters and Lange, 2015), using plagioclase rims and groundmass glass compositions as inputs. This method is viable because the groundmass glass at Nisyros-Yali is mostly unaffected by the eruption-triggering mingling events. Also, as presented above, the plagioclase rims are not affected by late-stage syn-eruptive crystallization. Moreover, the plagioclase-melt equilibrium test based on the Ab-An exchange coefficient (Putirka, 2008) suggests that most of the preserved low-An plagioclase rims are in equilibrium with the groundmass glass in each unit (Supplementary Fig. S4). In order to keep a conservative approach, we use a range of rim compositions that

cover a variation of at least 10% molar XAn and we pair each rim with each individual glass analysis. Hence, we obtain a range of dissolved water content for each deposit. We use the pre-recharge storage temperatures to define the conditions of plagioclase-melt equilibrium, because these temperatures were prevalent during plagioclase growth.

(iii) Melt viscosity, which depends on composition, temperature and dissolved water content is another critical parameter in influencing the eruptive style of a volcano. For example, higher melt viscosities enhance the fragmentation potential of the magma by increasing the dissipation time of stress (e.g. Dingwell, 1996; Papale, 1999). On the other hand, lower viscosities hinder fragmentation by allowing gas bubbles to move more readily, connect and outgas (e.g. Ruprecht and Bachmann, 2010). We need to estimate potential viscosity differences relevant for the feedbacks occurring during conduit ascent. Hence, we estimate the post-recharge, syn-eruptive melt viscosities using a numerical approach (Giordano et al., 2008). The calculation is based on the average groundmass glass composition, average eruptive temperature (derived from Fe-Ti oxides) and estimated dissolved water content for each unit. The effect of crystals is not considered, because it does not contribute to melt viscosity, but only to bulk viscosity.

(iv) We determine storage pressures by using the iteration of Anderson and Smith (1995). It is based on the same plagioclase-amphibole pairs used to determine storage tempera- tures and it follows the same reasoning. More details on applying the thermometers, barometers and hygrometers are given in Section C of the Supplementary text.

Pre-eruptive reservoir conditions

At Nisyros-Yali there is no correlation between eruptive temperatures and eruptive styles (Fig. 9A). Both eruption styles are triggered by magmas with eruptive temperatures in the range of 800-850˚C, but also by hotter magmas with temperatures between 900 and 950˚C. This comes in contrast with the example of Quizapu, where the effusive eruption was hotter (Ruprecht and Bachmann, 2010). At Nisyros-Yali, relatively cool magmas with a high expected viscosity generate effusive outpourings of lava, while hotter magmas can be explosive. For example, the hottest eruption of the series, the Upper Yali (~940˚C) behaves explosively.

On the other hand, the pre-recharge storage temperatures provide a significant difference between the conditions preceding effusive and explosive eruptions. With the exception of the older and less evolved Emborios dacite, the pre-recharge storage temperatures at Nisyros-Yali were colder before effusive eruptions (710-790˚C) when compared to their explosive counterparts (815-850˚C) (Fig. 9A).

Consequently, the pre-eruptive reheating was generally higher for the effusive eruptions. For example, the reservoir was heated by 40-120˚C before effusive events were triggered, compared to 10-30˚C before explosive events took place. This is similar to the case of Quizapu (Ruprecht and Bachmann, 2010), with the difference that the storage temperatures are the main variables at Nisyros-Yali. The main exception is the Upper Yali Pumice, which underwent c. 90˚C of heating. However, its storage temperature is still significantly higher when compared to the Yali effusive unit (~850˚C compared to ~710˚C). It appears to be a connection between storage temperatures and eruptive styles.

The generally colder populations of amphibole and plagioclase from effusive eruptions yield dissolved water contents of 5.6-6.5 wt%, while the explosive units return H_2O contents of 4.2-4.6 wt% (Fig. 9B). The results correlate well with the higher degree of differentiation of effusive units. They suggest that lava extrusions at Nisyros-Yali were generated by magmas with higher dissolved volatile contents than in the case of explosive eruptions. The exception here are the Emborios dacitic domes, recording the lowest H_2O concentration of the series (~3.5 wt%), correlated with a higher storage temperature and a lesser degree of differentiation.

The effusive units record eruptive melt viscosities between 3.5 and 4.5 log(η) ($10^{3.5}$-$10^{4.5}$ Pa s), while the explosive units generally record higher eruptive melt viscosities between 4.6 and 5.1 log(η) (Fig. 9C). These differences are apparent from units 2-to-7, despite the magmas having similar melt compositions and similar eruptive temperatures. It highlights the dominant influence of dissolved water contents on melt viscosities in this system. In the case of the hot Upper Yali Pumice, the large eruptive temperature induces a low melt viscosity, similar in value to what is estimated for effusive units. Therefore, in addition to the drop in melt viscosity, there has to be another key factor contributing to effusive-explosive transitions at this volcanic area.

The storage pressure estimates of the Nisyros-Yali rhyolitic magmas are mostly clustered in the range of 1.5–2 kbar for both effusive and explosive events (Fig. 9D). A striking difference is seen in unit 6, the Post-caldera domes, which records pressures in the range of 4-6 kbar. However, in this particular unit, the Al_2O_3 of amphiboles increases with Mg#, suggesting that the amphibole compositions are strongly influenced by changes in magma chemistry. It has been shown that amphibole chemistry is more sensitive to changes in melt chemistry than to pressure changes (Putirka, 2016). As a result, a chemical evolution of a system towards more primitive compositions (inverse differentiation) will erroneously increase the pressure estimates of amphibole barometry (Erdmann et al., 2014). Hence, the amphiboles found in the Post-caldera domes are not reliable pressure indicators.

At these subvolcanic storage depths (~ 6-8 km), Nisyros-Yali magmas can be gas saturated at >5 wt% H_2O. For example, by varying the CO_2 contents between 100-200 ppm (reasonable for Kos-Nisyros, Bachmann et al., 2010) and by varying the pressure between 1.5-2 kbar, we can estimate the potential water saturation field for Nisyros-Yali at between 5-6.5 wt% water (Newman and Lowenstern, 2002). The estimated dissolved water content for most effusive units is buffered at >5.6 wt%, indicating that this might be a more precise water saturation level. The higher dissolved water contents estimated for the Yali Obsidian could imply that the saturation level was higher in this specific case. This can be an effect of the extremely differentiated nature of the melt and of potentially lower CO_2 levels that concur to increase the water saturation limit (Newman and Lowenstern, 2002).

For the calculated pressures, all effusive units appear to have been saturated with a fluid/gas phase, except the Emborios Domes (which were clearly water undersaturated). In contrast, magmas feeding explosive events were undersaturated or close to saturation, and likely contained only minor amounts of exsolved volatiles. This leads to the seemingly counter-intuitive interpretation that the wetter magmas were the least explosive. However, as discussed below, the presence of *exsolved fluids* ("gas bubbles") in the magma chamber should indeed decrease the explosivity (see Degruyter et al., 2017).

Controls on eruptive styles.

Our data suggests that mafic recharge interacted with magmas kept under different storage conditions to generate different eruptive styles. The main differences are in the degree of differentiation, storage temperature, dissolved water content and potentially in the presence or abundance of an exsolved magmatic volatile phase. Three distinct situations are identified in the rock record of Nisyros-Yali:

(i) Effusive eruptions are triggered when hot recharge interacts with volatile-undersaturated warm dacites (>850 ˚C) with low dissolved water content (c. 3.5 wt%) (e.g. Emborios);

(ii) Explosive events are triggered when hot recharge interacts with volatile-undersaturated and relatively warm rhyolites (>800˚C) with moderate dissolved water contents (c. 4.2-4.6 wt%); (e.g. Lower and Upper Pumice of Nisyros and Yali);

(iii) Effusive eruptions are triggered when hot recharge interacts with more differentiated, potentially volatile supersaturated, colder rhyolites (<800˚C for Nisyros and <750˚C for Yali) with high dissolved water contents (>5.6 wt%) (e.g. Nikia, Avlaki flows, Post-caldera and Yali Obsidian lava flows).

Based on this, there are at least two transition domains where the effusive-explosive shifts can occur. The shifts correlate with the increasing volatile concentrations of the melts. For example, in undersaturated conditions, an increase in dissolved water content favors the explosive behavior of magmas. This is valid up to the gas saturation threshold. As volatile supersaturation is reached, any further increase in the volatile budget promotes effusivity (see cartoon from Fig. 10). This observation is linked to volatiles exsolving in the reservoir during supersaturated differentiation, while the dissolved water content remains buffered.

To better understand how the effusive-explosive transition works in the water-supersaturated domain, we will evaluate some of the effects that exsolved fluids can have on the magma reservoir. There are two important points that need to be addressed: (i) the ability of the reservoir to effectively trap a significant amount of exsolved volatiles and (ii) the implications this has on recharge dynamics.

(i) It has been recently shown that through the formation of gas finger-channels, volatiles can migrate inside a mush system, but a fraction of at least 10-15 vol% remains trapped at any given time (Parmigiani et al., 2016). The most efficient outgassing is constrained to the intermediate crystallinity areas of the mush: ~ 40-70 vol% crystals (Parmigiani et al., 2017). Long-lived mush systems, like that of Kos-Nisyros-Yali, typically contain gradients in crystal content: crystal-rich areas can host smaller pockets of low-crystallinity evolved melt that are eruptible (Bachmann and Huber, 2016). These crystal poor, eruptible areas will accumulate the gas bubbles due to finger-channel breakage (Parmigiani et al., 2016). In the crystal-poor environment, the exsolved volatiles are less able to escape due to bubble-liquid and bubble-bubble interactions (Faroughi et al., 2014; Parmigiani et al., 2016). Therefore, the eruptible areas of the mush are efficient at trapping and accumulating a fraction of the gas bubbles.

(ii) Exsolved volatiles can increase the bulk compressibility of the host reservoir (Huppert and Woods, 2002; Edmonds and Wallace, 2017; Degruyter et al., 2017; Edmonds and Woods, 2018). Basically, the volume of exsolved gas adjusts more readily to pressure changes than the volume of other phases present in the magma (higher bulk compressibility). The gas

bubbles can reduce their volume as a result of pressure increase, or can partly re-dissolve in a dynamic, responsive way, as the gas saturation limit changes. This happens when the pressure increases, for example in the case of recharge. In other words, exsolved volatiles have a cushioning effect. Because of this, during a recharge event, the exsolved volatiles have the potential to neutralize a part of the magma chamber overpressure caused by the addition of recharge mass (Degruyter et al., 2017). This delays the triggering of the eruption (Degruyter et al., 2016). The volume reduction of the gas phase allows for a higher fraction of recharge melt to be accommodated in the volatile-supersaturated reservoir, which in turn allows for more heat transfer to occur before magma ascent begins (Degruyter et al., 2017).

In summary, we argue that significant amounts of fluids ("gas bubbles") generated at Nisyros-Yali are likely to remain trapped within the eruptible areas of the mush. Moreover, the exsolved volatiles will delay recharge-triggered eruptions through their ability to compress and re-dissolve. This feedback explains the efficient pre-eruptive heating of gas-supersaturated reservoirs producing effusive eruptions. The heating drives the viscosity to lower values, contributing to the effusive behavior. Only the Upper Yali event behaves differently, by erupting explosively under low viscosity conditions. This means that, in addition to reheating and viscosity reduction, there is an additional control to effusive-explosive transitions. Hence, we propose a similar but complementary hypothesis to that of Degruyter et al., (2017), which explains the effusive-explosive transitions at Nisyros-Yali, including the mentioned exception:

> Stage 1 (in magma reservoir): Recharge material is injected in a gas supersaturated upper crustal mush. Under the pressure increase generated by this injection, the exsolved volatiles will actively compress. The pressure increase will also push up the gas saturation limit, which determines the gas bubbles to partly re-dissolve in the melt. This happens under disequilibrium conditions (*i.e.* the pressure increase is not caused by normal lithostatic load). This creates additional space to accommodate a higher fraction of hot material, to which the exsolved volatiles respond by compressing and dissolving even more. This delays the eruption until the volume reduction caused by the compressibility and dissolution of gas is overwhelmed by the volumes of recharge melt. By this point, the feedback has allowed for more heating to occur than in the absence of the exsolved phase, and it allowed for a larger viscosity drop.
>
> Stage 2 (in conduit): When the eruption is finally triggered, the depressurizing wave allows the previously re-dissolved volatiles (re-dissolved under disequilibrium conditions) to re-nucleate *en-masse*. Under lower-viscosity conditions and massive nucleation, early coalescence and expansion will occur. It will foster the development of a permeable foam at the onset of magma ascent. In other words, the early availability of gas bubbles associated with the drop in melt viscosity enhances the development of gas permeability during conduit ascent. In turn, it leads to more efficient outgassing and to neutralizing the explosive potential of the magma.

This mechanism allows the water-rich, supersaturated magmas at Nisyros-Yali to lose gas more efficiently than their undersaturated (or poorly saturated) counterparts. This can explain how effusive eruptions are generated despite having higher initial volatile contents. In addition, this mechanism highlights that the role of the exsolved volatiles in influencing

effusive-explosive transitions is not limited to increasing the compressibility in the magma chamber (see stage 1). For example, the presence of early exsolved volatiles at the onset of magma ascent seems to be at least as important as the viscosity drop associated to reheating (see stage 2). The Upper Yali is a good case for this discussion. It is the least voluminous deposit of the investigated series, with a thickness of about 3 m, compared to the almost 150 m thick Lower Yali deposit. This reflects a low-volume eruptible melt pocket that is easily overwhelmed by the recharge volume. The high volumetric ratio of recharge/resident melt can explain the large pre-eruptive reheating observed in the Upper Yali. In this case, the large reheating does not require gas supersaturation. Still, in the absence of the early exsolved volatiles, the magma behaves explosively despite the significant viscosity drop. The exsolved volatiles build via first boiling during conduit ascent, and there is insufficient time to create a permeable framework that allows sufficient outgassing.

The model described above can theoretically be time-dependent, space-dependent or more likely, a combination of both. In a time-dependent scenario, the same area of the mush is being tapped by the recharge melts at different stages of the cooling-fractionation-exsolution-eruption-reheating cycle (Fig. 11A). The eruptive style becomes a function of whether a major recharge occurs when the system is gas undersaturated or supersaturated. In the space-dependent scenario, bubble-poor and bubble-rich areas coexist at the same time in the mush. The eruptive style becomes a more random-function of which area is tapped by the major recharge (Fig 11B).

CONCLUSIONS AND FUTURE DIRECTIONS.

Compared to explosive eruptions, effusive events at Nisyros-Yali generally record colder storage temperatures, higher amounts of pre-eruptive reheating and higher volatile contents. A key finding is that the magmas generating effusive events appear to have been supersaturated with a fluid phase in the reservoir, while the magmas involved in explosive eruptions were not. Hence, the presence versus absence, or abundance versus scarcity of exsolved volatiles in the magma reservoir seem to be the key to effusive-explosive transitions at this volcanic system. We suggest that effusivity is promoted by fluid exsolution in the magma chamber. In other words, *exsolved* volatiles in the magma chamber appear to have the opposite effect to *dissolved* volatiles in mechanically controlling eruptive style.

This observation highlights the importance of further studies to evaluate the gas supersaturated versus undersaturated quality of the magmas. A direct confirmation of the presence of a fluid phase in the magma chamber is challenging to achieve based on the erupted rock record. There is no proven method to petrologically determine whether a magma actually contained a fluid phase (and if so, how much), although there are pioneering papers that need to be tested against more natural systems (Balcone-Boissard et al., 2008; Webster et al., 2015; Stock et al., 2016). This is currently work in progress for Nisyros-Yali. The results of such investigations can confirm our hypothesis, which is based around a comparative dataset of effusive-explosive deposits and constrained by physical controls explored in recently published numerical models.

In essence, we propose that the interplay between differentiation and magma recharge in volcanoes can influence eruptive styles. We can consider a time-dependent model, where all eruptible areas of the mush share similar properties at a given moment in time. Alternatively, we can consider a space-dependent model where the eruptible areas of the mush have

different properties at the same moment in time. Either way, the mechanical controls on eruptive styles are similar. To exemplify, we consider a time-dependent model:

> I – Effusive events. During dormancy magma reservoirs cool, differentiate, and increase the volatile content up to reaching volatile supersaturation. This has an (i) indirect and a (ii) direct effect on eruptive style. Firstly, (i) magma reservoirs become more compressible and can host higher fractions of recharge melt. In effect, they are more efficiently heated by recharge, which leads to a significant drop in melt viscosity. Also, it leads to an increase in magma chamber pressure that partly re-dissolves the volatiles. Secondly, once magma ascent is triggered, (ii) gas bubbles will improve further exsolution by heterogeneous nucleation (Hurwitz and Navon, 1994), while the previously re-dissolved volatiles will re-nucleate *en-masse* to develop an early permeable foam. Low melt viscosities combined with the presence of an early gas phase enhance conduit outgassing and lead to effusive outpourings, thus controlling the eruptive style. However, a reduction in melt viscosity in the absence of exsolved volatiles in the magma chamber might still lead to an explosive event (*i.e.* Upper Yali case).
>
> II – Explosive events. Whatever the style of the first eruption is, it leaves behind a degassed and depressurized system. It is subsequently replenished and reheated by the recharge melts. It resumes cooling and rebuilding its volatile content via differentiation. However, if a new major recharge takes place before volatile supersaturation is reached (or before building a significant volume of exsolved gas), the magma chamber pressurizes more readily. Hence, an eruption is triggered by smaller volumes of recharge melt. Heating is less efficient. Moreover, the permeable foam is not available early-on due to the lack of previously exsolved bubbles. Therefore, bubble nucleation starts in the conduit during magma ascent and permeability development is reduced, slowing down gas discharge. Although the dissolved volatile content is lower than in the effusive case, an explosive eruption will likely occur.

If proven correct, our hypothesis can potentially aid volcanic monitoring and eruption forecast efforts in cases where magmatic systems behave similarly to Nisyros-Yali. This is especially relevant for volcanoes where a time dependency is observed between distinct effusive and explosive events. Furthermore, this concept can explain several less intuitive cycles in eruptive dynamics. For example, in several volcanic arcs involving water-rich, silicic magmas, eruption cycles can ***start*** with effusive events, and can be followed by explosive eruptions, sometimes larger than the precursor lava outpouring. Well-described examples include the Pagosa Peak dacite – Fish Canyon Tuff sequence (Bachmann et al., 2000), the Cleetwood Flow and Crater Lake ignimbrite (Bacon and Lanphere, 2006) and the Quizapu 1846-47 and 1932 eruption (Ruprecht and Bachmann, 2010). This is an attractive concept for the case of Nisyros-Yali and exploring it at other volcanoes of fluctuating eruptive style would help to develop a general model to understand this crucial transition.

REFERENCES.

Allen S.R., McPhie J., 2000. Water-settling and resedimentation of submarine rhyolitic pumice at Yali, eastern Aegean, Greece. Journal of Volcanology and Geothermal Research, 95, 285-307.

Anderson, J. L., Smith, D. R., 1995. The effect of temperature and oxygen fugacity on Al-in-hornblende barometry. American Mineralogist, 80, 549-59.

Bachmann, O., Deering, C.D., Ruprecht, J.S., Huber, C., Skopelitis, A., Schnyder, C., 2012. Evolution of silicic magmas in the Kos-Nisyros volcanic center, Greece: a petrological cycle associated with caldera collapse. Contributions in Mineralogy and Petrology, 163, 151-166.

Bachmann, O., Dungan, M.A., Lipman, P.W., 2000. Voluminous lava-like precursor to a major ash-flow tuff: low-column pyroclastic eruption of the Pagosa Peak Dacite, San Juan volcanic field, Colorado. Journal of Volcanology and Geothermal Research, 98, 153-171.

Bachmann, O., Huber, C., 2016. Silicic magma reservoirs in the Earth's crust. American Mineralogist, 101, 2377-2404.

Bachmann, O., Wallace, P.J., Bourquin, J., 2010. The melt inclusion record from the rhyolitic Kos Plateau Tuff (Aegean Arc). Contributions to Mineralogy and Petrology, 159, 187-202.

Bachmann, O., Allen, S.R., Bouvet de Maisonneuve, C., 2019. The Kos-Nisyros-Yali Volcanic Field. Elements 15, 191–196.

Bacon, C.R., Hirschmann, M.M., 1988. Mg/Mn partitioning as a test for equilibrium between coexisting Fe-Ti oxides. American Mineralogist, 73, 57-61.

Bacon, C.R., Lanphere, M.A., 2006. Eruptive history and geochronology of Mount Mazama and the Crater Lake region, Oregon. Geological Society of America Bulletin, 118, 1331-1359.

Baker, D.R., 2008. The fidelity of melt inclusions as records of melt composition. Contributions to Mineralogy and Petrology, 156, 377-395.

Balcone-Boissard, H., Villemant, B., Boudon, G., Michel, A., 2008. Non-volatile vs volatile behaviours of halogens during the AD 79 plinian eruption of Mt. Vesuvius, Italy. Earth and Planetary Science Letters, 269, 66-79.

Bini, G., Chiodini, G., Cardellini, C., Vougioukalakis, G.E., Bachmann, O., 2019. Diffuse emission of CO2 and convective heat release at Nisyros caldera (Greece). J. Volcanol. Geotherm. Res. 376, 44–53.

Braschi, E., Francalanci, L., Vougioukalakis, G.E., 2012. Inverse differentiation pathway by multiple mafic magma refilling in the last magmatic activity of Nisyros Volcano, Greece. Bulletin of Volcanology, 74, 1083-1100.

Browne, B.L., Gardner, J.E., 2006. The influence of magma ascent path on texture, mineralogy and formation of hornblende reaction rims. Earth and Planetary Science Letters, 246, 161-176.

Bucholz, C.E., Gaetani, G.A., Behn, M.D., Shimizu, N., 2013. Post-entrapment modification of volatiles and oxygen fugacity in olivine-hosted melt inclusions. Earth and Planetary Science Letters, 374, 145-155.

Cashman, K.V., Sparks, R.S.J., Blundy, J., 2017. Vertically extensive and unstable magmatic systems: A unified view of igneous processes. Science, 355, 1280.

Cassidy, M., Castro, J.M., Helo, C., Troll, V.R., Deegan, F.M., Muir, D., Neave, D.A., Mueller, S.P., 2016. Volatile dilution during magma injections and implications for volcano explosivity. Geology, 44, 1027-1030.

Cassidy, M., Manga, M., Cashman, K., Bachmann, O., 2018. Controls on explosive-effusive volcanic eruption styles. Nature Communications, 9:2839, DOI: 10.1038/s41467-018-05293-3.

Castro, J.M., Cordonnier, B., Tuffen, H., Tobin, M.J., Puskar, L., Martin, M.C., Bechtel, H.A., 2012. The role of melt-fracture degassing in defusing explosive rhyolite eruptions at volcán Chaitén. Earth and Planetary Science Letters, 333-334, 63-69.

Chiodini, G., Brombach, T., Caliro, S., Cardellini, C., Marini, L., Dietrich, V., 2002. Geochemical indicators of possible ongoing volcanic unrest at Nisyros Island (Greece). Geophys. Res. Lett. 29. https://doi.org/10.1029/2001GL014355.

Degruyter, W., Bachmann, O., Burgiser, A., Manga, M., 2012. The effects of outgassing on the transition between effusive and explosive silicic eruptions. Earth and Planetary Science Letters, 349-350, 161-170.

Degruyter, W., Huber, C., Bachmann, O., Cooper, K.M., Kent, A.J.R., 2016. Magma reservoir response to transient recharge events: The case of Santorini volcano (Greece). Geology, 44, 23-26.

Degruyter, W., Huber, C., Bachmann, O., Cooper, K.M., Kent, A.J.R., 2017. Influence of exsolved volatiles on reheating silicic magmas by recharge and consequences for eruptive style at Volcan Quizapu (Chile). Geochemistry, Geophysics, Geosystems, DOI 10.1002/2017GC007219.

Di Genova, D., Kolzenburg, S., Wiesmaier, S., Dallanave, R., Neuville, D.R., Hess, K.U., Dingwell, D.B., 2017. A compositional tipping point governing the mobilization and eruptive style of rhyolitic magma. Nature, 552, 235-238.

Di Paola, G.M., 1974. Volcanology and Petrology of Nisyros (Dodecanese, Greece). Bulletin of Volcanology, 38, 944-987.

Dietrich, V.J., Lagios, E., (Eds.), 2017. Nisyros Volcano. Springer, 468 pp.

Dietrich, V.J., Popa, R-G., 2017. Petrology and Geochemistry of Lavas and Pyroclastics. In: Dietrich, V.J., Lagios, E., (Eds.), Nisyros Volcano, Springer, 103-144.

Dingwell, D.B., 1996. Volcanic Dilemma: Flow or Blow?: Science, 273, 1054-1055.

Edmonds, M., Herd, R., 2007. A volcanic degassing event at the explosive-effusive transition. Geophysical Research Letters, 34, doi: 10.1029/2007GL031379.

Edmonds, M., Wallace, P.J., 2017. Volatiles and Exsolved Vapor in Volcanic Systems. Elements, 13, 29-34.

Edmonds, M., Woods, A.W., 2018. Exsolved volatiles in magma reservoirs. Journal of Volcanology and Geothermal Research, 368, 13-30.

Eichelberger, J.C., Carrigan, C.R., Westrich, H.R., Price, R.H., 1986. Non-explosive silicic volcanism. Nature, 323, 598-602.

Erdmann, S., Martel, C., Pichavant, M., Kushnir, A., 2014. Amphibole as an archivist of magmatic crystallization conditions: problems, potential, and implications for inferring magma storage prior to the paroxysmal 2010 eruption of Mount Merapi, Indonesia. Contributions to Mineralogy and Petrology, 167, DOI 10.1007/s00410-014-1016-4.

Faroughi, S.A., Huber, C., 2014. Unifying the relative hindered velocity in suspensions and emulsions of nondeformable particles. Geophysical Research Letters, 42, 53-59.

Forni, F., Bachmann, O., Mollo, S., De Astis, G., Gelman, S.E., Elli, B.S., 2016. The origin of a zoned ignimbrite: Insights into the Campanian Ignimbrite magma chamber (Campi Flegrei, Italy). Earth and Planetary Science Letters, 449, 259-271.

Francalanci, L., Varekamp, J.C., Vougioukalakis, G., Defant, M.J., Innocenti, F., Manetti, P., 1995. Crystal retention, fractionation and crustal assimilation in a convecting magma chamber, Nisyros Volcano, Greece. Bulletin of Volcanology, 56, 601-620.

Gaetani, G.A., O'Leary, J.A., Shimizu, N., Bucholz, C.E., Newville, M., 2012. Rapid reequilibration of H2O and oxygen fugacity in olivine-hosted melt inclusions. Geology, 40, 915-918.

Gardner, J.E., 2009. The impact of pre-existing gas on the ascent of explosively erupted magma. Bull. Volcanol. 71, 835–844.

Ghiorso, M.S., Evans, B.W., 2008. Thermodynamics of Rhombohedral Oxide Solid Solutions and a Revision of the Fe-Ti Two-oxide Geothermometer and Oxygen-barometer. American Journal of Science, 308, 957-1039.

Gill, R., 2010. Igneous Rocks and Processes. Wiley-Blackwell, 428 pp.

Giordano, D., Russel, J.K., Dingwell, D.B., 2008. Viscosity of magmatic liquids: a model. Earth and Planetary Science Letters, 271, 123-134.

Gonnermann, H.M., Manga, M., 2003. Explosive volcanism may not be an inevitable consequence of magma fragmentation. Nature, 426, 432-435.

Gonnermann, H.M., Manga, M., 2013. Dynamics of magma ascent in the volcanic conduit. In: Fagents, S.A., Gregg, T.K.P, Lopes, R.M.C. (eds.) Modeling Volcanic Processes, Cambridge University Press, 55-84.

Graham, C.M., Harmon, R.S., Sheppard, S.M.F., 1984. Experimental hydrogen isotope studies: hydrogen isotope exchange between amphibole and water. American Mineralogist, 69, 128-138.

Guillong, M., Meier, D., Allan, M., Heinrich, C., Yardley, B., 2008. SILLS: a MATLAB-based program for the reduction of laser ablation ICP-MS data of homogeneous materials and inclusions. In: Sylvester, P. (ed.) Laser Ablation ICP–MS in the Earth Sciences: Current Practices and Outstanding Issues. Mineralogical Association of Canada, Short Course Series. Vancouver, 328–333.

Guillong, M., von Quadt, A., Sakata, S., Peytcheva, I., Bachmann, O., 2014. LA-ICP-MS Pb–U dating of young zircons from the Kos–Nisyros volcanic centre, SE Aegean arc. J. Anal. At. Spectrom. 29, 963–970.

Guillong, M., Sliwinski, J.Y., Schmitt, A., Forni, F., Bachmann, O., 2016. U-Th zircon dating by laser ablation single collector inductively coupled plasma-mass spectrometry (LA-ICP-MS). Geostand. Geoanal. Res. 40, 377–387.

Holland, T., Blundy, J., 1994. Non-ideal interactions in calcic amphiboles and their bearing on amphibole-plagioclase thermometry. Contributions to Mineralogy and Petrology, 116, 433-447.

Huppert, H.E., Woods, A.W., 2002. The role of volatiles in magma chamber dynamics. Nature, 420, 493-495.

Hurwitz, S., Navon, O., 1994. Bubble nucleation in rhyolitic melts: Experiments at high pressure, temperature, and water content. Earth and Planetary Science Letters, 122, 267-280

Klaver, M., Matveev, S., Berndt, J., Lissenberg, C.J., Vroon, P.Z., 2017. A mineral and cumu- late perspective to magma differentiation at Nisyros volcano, Aegean arc. Contrib. Mineral. Petrol. 172, 95.

Klaver, M., Blundy, J.D., Vroon, P.Z., 2018. Generation of arc rhyodacites through cumulate-melt reactions in a deep crustal hot zone: Evidence from Nisyros volcano. Earth and Planetary Science Letters, 497, 169-180.

Klug, C., Cashman, K.V., 1996. Permeability development in vesiculating magmas: implications for fragmentation. Bulletin of Volcanology, 58, 87-100.

Koleszar, A.M., Kent, A.J.R., Wallace, P.J., Scott, W.E., 2012. Controls on long-term low explosivity at andesitic arc volcanoes: Insights from Mount Hood, Oregon. Journal of Volcanology and Geothermal Research, 219-220, 1-14.

Lee, C.A., Bachmann, O., 2014. How important is the role of crystal fractionation in making intermediate magmas? Insights from Zr and P systematics. Earth and Planetary Science Letters, 393, 266-274.

Longchamp, C., Bonadonna, C., Bachmann, O., Skopelitis, A., 2011. Characterization of tephra deposits with limited exposure: the example of two largest explosive eruptions at nisyros volcano (Greece). Bulletin of Volcanology, 73, 1337-1352.

Marxer, F., Ulmer, P., 2019. Crystallisation and zircon saturation of calc-alkaline tonalite from the Adamello Batholith at upper crustal conditions: an experimental study. Contrib. Mineral. Petrol. (in press).

Morrissey, M., Zimanowski, B, Wohletz, K., Buettner, R., 2000. Phreatomagmatic Fragmentation. In: Sigurdsson, H., Houghton, B., McNutt, S.R., Rymer, H., Stix, J., (Eds.), Encyclopedia of Volcanoes, Academic Press, 431-446.

National Academies of Sciences, Engineering, and Medicine, 2017. Volcanic Eruptions and Their Repose, Unrest, Precursors, and Timing. The National Academies Press, Washington DC, 122 pp.

Newman, S., Lowenstern, J.B., 2002. VolatileCalc: a silicate melt-H2O-CO2 solution model written in Visual Basic for excel. Computers & Geosciences, 28, 597-604.

Nguyen, C.T., Gonnermann, H.M., Houghton, B.F., 2014. Explosive to effusive transition during the largest volcanic eruption of the 20th century (Novarupta 1912, Alaska). Geology, 42, 703-706.

Oldenburg, C.M., Spera, F.J., Yuen, D.A., Sewell, G., 1989. Dynamic mixing in magma bodies: Theory, simulations, and implications. Journal of Geophysical Research, 94, 9215-9236.

Papale, P., 1999. Strain-induced magma fragmentation in explosive eruptions. Nature, 397, 425-428.

Parfitt, E.A., Wilson, L., 2008. Fundamentals of Physical Volcanology. Blackwell, Oxford, 256 pp.

Parmigiani, A., Degruyter, W., Leclaire, S., Huber, C., Bachmann, O., 2017. The mechanics of shallow magma reservoir outgassing. Geochemistry, Geophysics, Geosystems, 18, 2887-2905.

Parmigiani, A., Faroughi, S., Huber, C., Bachmann, O., Y, Su., 2016. Bubble accumulation and its role in the evolution of magma reservoirs in the upper crust. Nature, 532, 492-495.

Pe-Piper, G., Piper, D.J.W., 2005. The South Aegean active volcanic arc: relationships between magmatism and tectonics. Developments in Volcanology. vol. 7, pp. 113–133.

Pollaci, M., Rosi, M., Landi, P., Di Muro, A., Papale, P., 2005. Novel interpretation for Shift between Eruptive Styles in Some Volcanoes. EOS, 86, 333-340.

Putirka, K., 2008. Thermometers and Barometers for Volcanic Systems. In: Putirka, K., Tepley, F., (Eds.), Minerals, Inclusions and Volcanic Processes, Reviews in Mineralogy and Geochemistry, Mineralogical Society of America, 69, 61-120.

Putirka, K., 2016. Amphibole thermometers and barometers for igneous systems, and some implications for eruption mechanisms of felsic magmas at arc volcanoes. American Mineralogist, 101, 841-858.

Rehren, T., 1988. Geochemie und Petrologie von Nisyros (Östliche Ägäis). University of Freiburg, p. 167.

Rowe, M.C., Ellis, B.S., Lindeberg, A., 2012. Quantifying crystallization and devitrification of rhyolites by means of X-ray diffraction and electron microprobe analysis. American Mineralogist, 97, 1685–1699.

Ruprecht, P., Bachmann, O., 2010. Pre-eruptive reheating during magma mixing at Quizapu volcano and the implications for the explosiveness of silicic arc volcanoes. Geology, 38, 919-922.

Rutherford, M.J., Devine, J.D., 2003. Magmatic conditions and magma ascent as indicated by hornblende phase equilibria and reactions in the 1995–2002 Soufriere Hills magma. J. Petrol. 44, 1433–1454.

Rutherford, M.J., Hill, P.M., 1993. Magma ascent rates from amphibole breakdown: an experimental study applied to the 1980-1986 Mount St. Helens eruptions. Journal of Geophysical Research: Solid Earth, 98, 19667-19685.

Seymour, K., Vlassopoulos, D., 1989. The potential for future explosive volcanism associated with dome growth at Nisyros, Aegean volcanic arc, Greece. J. Volcanol. Geotherm. Res. 37, 351–364.

Spera, F.J., Schmidt, J.S., Bohrson, W.D., Brown, G.A., 2016. Dynamics and thermodynamics of magma mixing: Insights from a simple exploratory model. American Mineralogist, 101, 627-643.

Steele-Macinnis, M., Esposito, R., Bodnar, R.J., 2011. Thermodynamic model for the effect of post-entrapment crystallization on the H2O-CO2 systematics of vapor-saturated silicate melt inclusions. Journal of Petrology, 52, 2461-2482.

Stock, M.J., Humphreys, M.C.S., Smith, V.C., Isaia, R., Pyle, D.M., 2016. Late-stage volatile saturation as a potential trigger for explosive volcanic eruptions. Nature Geoscience, 9, 249-255.

Tomlinson, E.L., Kinvig, H.S., Smith, V.C., Blundy, J.D., Gottsmann, J., Müller, W., Menzies, M.A., 2012. The Upper and Lower Nisyros Pumices: revisions to the Mediterranean tephrostratigraphic record based on micron-beam glass geochemistry. J. Volcanol. Geotherm. Res. 243-244, 69–80.

Venezky, D., and Rutherford, M., 1999. Petrology and Fe-Ti oxide reequilibration of the 1991 Mount Unzen mixed magma. Journal of Volcanology and Geothermal Research, 89, 213–230.

Wallace, P.J., Kamenetsky, V.S., Cervantes, P., 2015. Melt inclusion CO2 contents, pressures of olivine crystallization, and the problem of shrinkage bubbles. American Mineralogist, 100, 787-794

Waters, L.E., Lange, R.A., 2015. An updated calibration of the plagioclase-liquid hygrometer-thermometer applicable to basalts through rhyolites. American Mineralogist, 100, 2172-2184.

Webster, J.D., Vetere, F, Botcharnikov, R.E., Goldoff, B., McBirney, A., Doherty, A.L., 2015. Experimental and modeled chlorine solubilities in aluminosilicate melts at 1 to 7000 bars and 700 to 1250˚C: Applications to magmas of Augustine Volcano, Alaska. American Mineralogist, 100, 522-535.

Woods, A.W., Koyaguchi, T., 1994. Transitions between explosive and effusive eruptions of silicic magmas. Nature, 370, 641-644.

ACKNOWLEDGEMENTS.

This research was partly funded through Swiss NSF # 200020_165501 to O. Bachmann. We would like to thank Prof. Dr. Volker Dietrich, Dr. Matthieu E. Galvez and Dr. James D. Webster for useful discussions and insights.

FIGURE CAPTIONS.

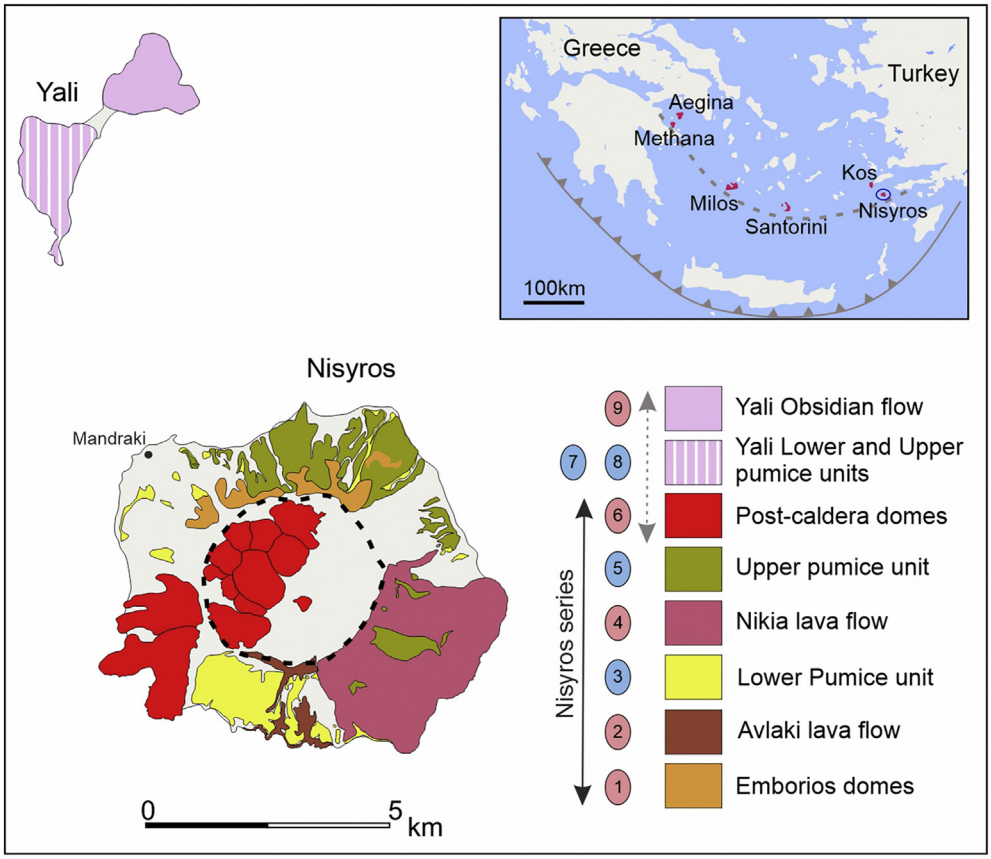

Fig. 1 Simplified geological map of Nisyros-Yali after Dietrich and Lagios (2017) highlighting the 9 investigated units. The relative age of the units has been slightly changed from that presented in the original map. Here, Emborios is considered older than Avlaki. There are no stratigraphic relations between these units, and no geochronology data. However, Emborios is less evolved than the rhyolitic eruptions, the mineral chemistry is distinct (see later in the paper) and, as opposed to Avlaki and the other rhyolitic deposits, Emborios erupted at a stage when zircons did not yet saturate in the Nisyros-Yali mush. Similarly, the age relation between the Yali events and the Post-caldera dome eruption on Nisyros is unclear (marked with a dashed arrow). The inset marks the location of Nisyros-Yali and gives an overview of the Aegean Sea with the main volcanic islands. The volcanic arc and the subduction front are sketched (after Pe-Piper and Piper, 2005).

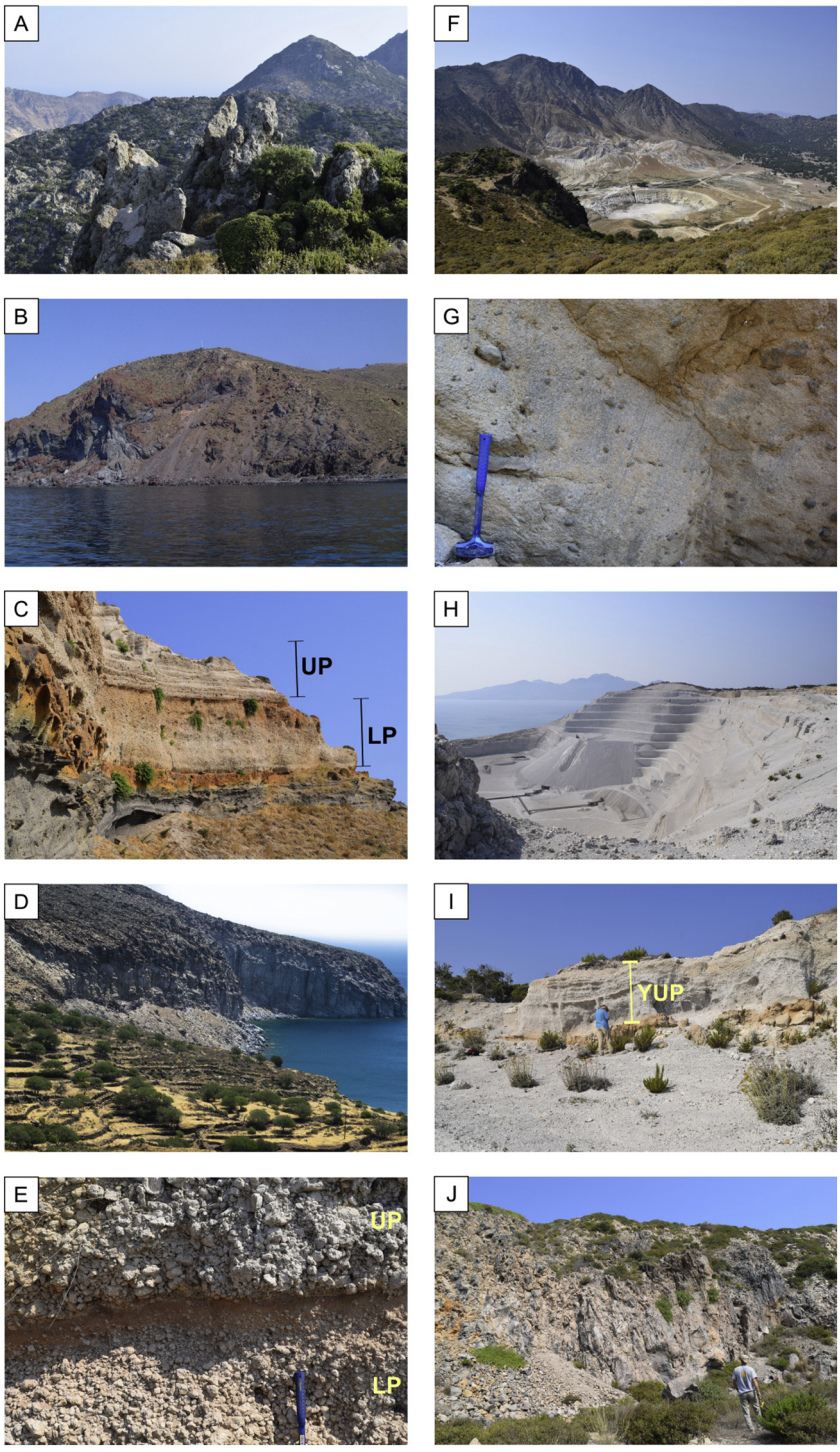

Fig. 2 Overview of the sampled units: (A) Emborios dome, (B) Avlaki lava flow, (C, E) Lower and Upper Pumice deposits, (D) Nikia lava flow (emplaced after the Lower, and before the Upper Pumice event), (F,G) Post-caldera domes, (H) Yali Lower Pumice (in open quarry), (I) Yali Upper Pumice and (J) Yali Obsidian flow. Photo (B) is courtesy of Prof. Dr. Volker Dietrich.

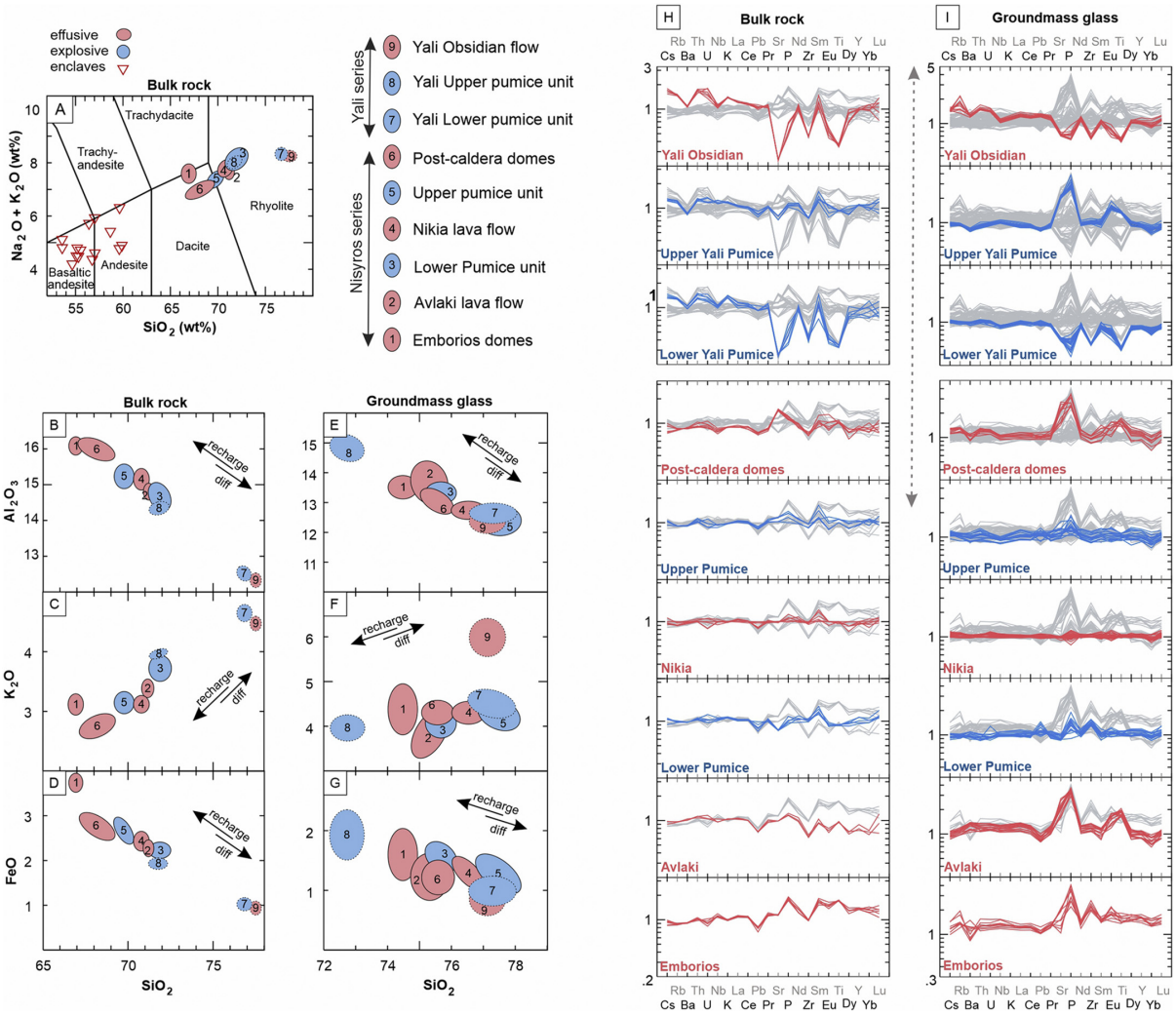

Fig. 3 Geochemical overview of effusive (red) and explosive (blue) deposits. (A): Bulk-rock TAS diagram showing the compositional fields of the units. Andesite and basaltic-andesite enclaves from lava flows and pumices are also plotted. (B, C, D): Harker diagrams showing WD-XRF bulk-rock and (E, F, G): calibrated SEM groundmass glass analyses of the 9 investigated units. The data is plotted using compositional fields. Magma recharge trends are marked by a decrease of SiO2 and increase in FeO and Al2O3. Differentiation has the opposite effect and leads to enrichment in K2O, which is incompatible in the Nisyros-Yali system. (H, I): Spider diagrams of LA-ICPMS data normalized to the composition of Nikia lava flow (unit 4). The diagrams depict the trace-element behavior of bulk rocks (H) and groundmass glasses (I). The data is shown sequentially, from the oldest unit (bottom) to the youngest unit (top). Note the general tendency of differentiation, which is reversed in the

Post-caldera domes and Upper Yali Pumice units. The age uncertainty between the Post-caldera domes and the Yali events is marked with a dashed arrow.

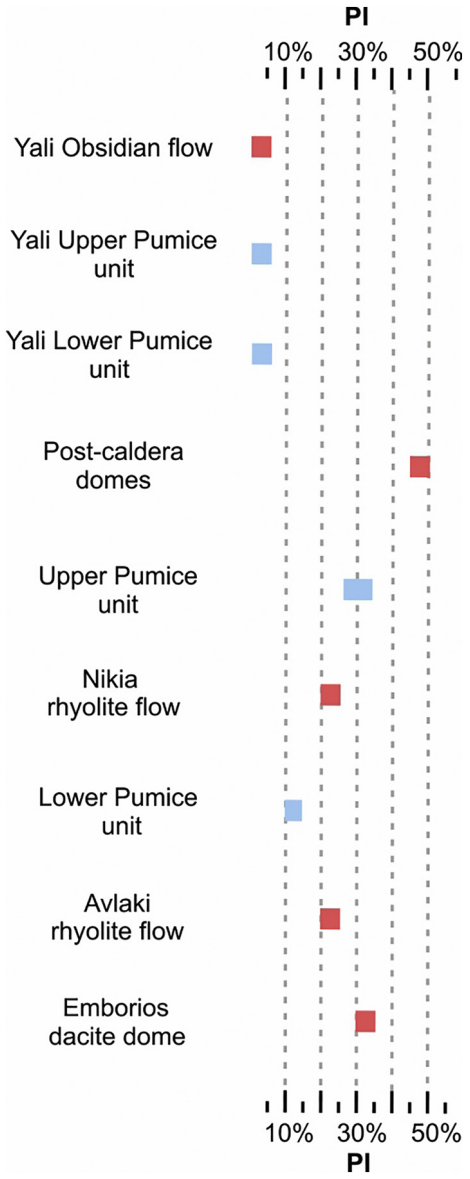

Fig. 4: Porphyritic index of effusive (red) and explosive (blue) units. The Yali events are generated by crystal-poor melts, while a wide PI variation is recorded in the Nisyros deposits. Based on crystallinity, there is no distinction between effusive and explosive eruptions.

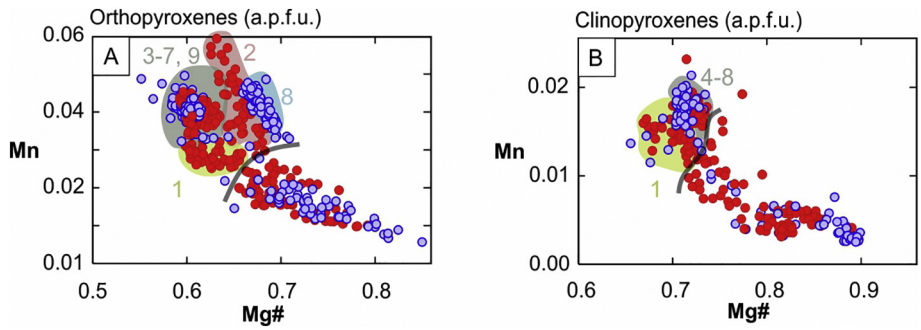

Fig. 5: EPMA orthopyroxene (A) and clinopyroxene (B) data. The colored compositional fields are marked with numbers as in Figure 1. In addition to the crystals originating in the mush system of Nisyros-Yali, the ubiquitous presence of unzoned, high-Mg# phenocrysts indicates a recharge component present in both effusive (red) and explosive (blue) deposits. The grey line visually separates the compositional fields of the mush crystals from the recharge crystals.

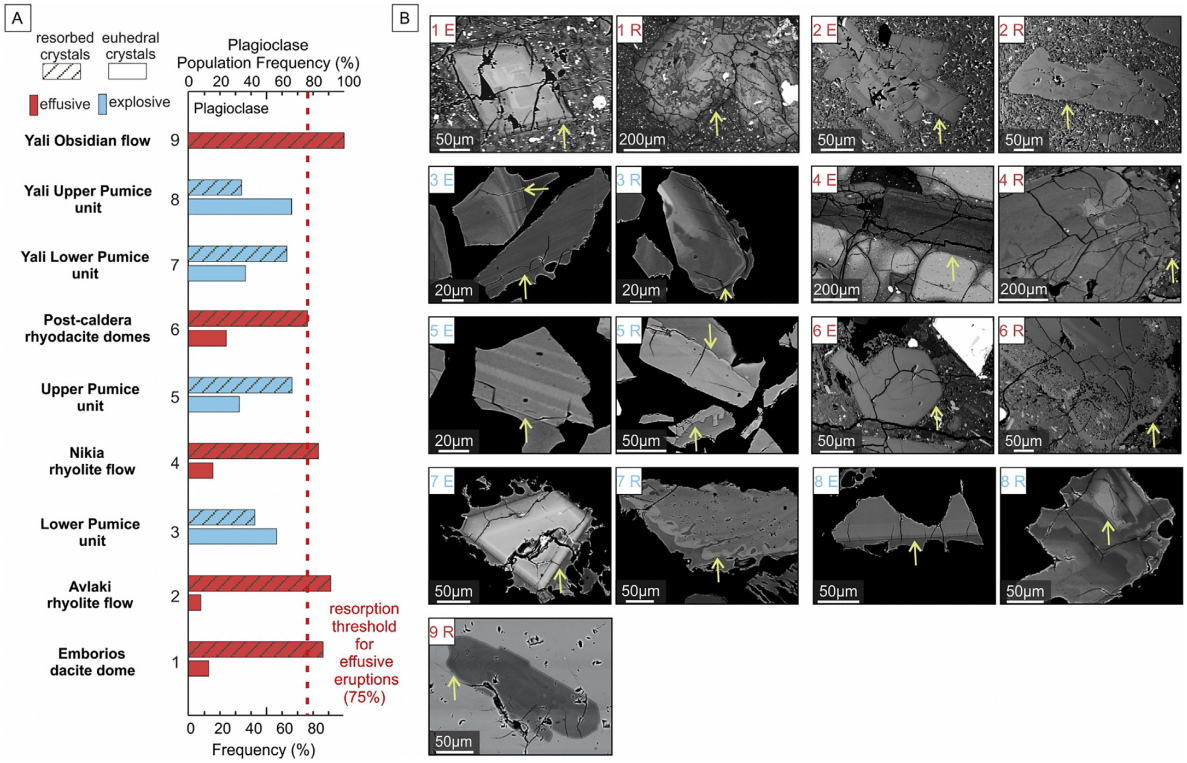

Fig. 6: Overview of plagioclase populations. (A): Frequency of resorbed and euhedral plagioclase populations, determined on a sample of 50-100 crystals per unit. (B): BSE images

of crystals reflecting the populations present in each unit. The images are numbered according to the unit (*e.g.* 1 is Emborios and 9 is the Yali Obsidian), marked as euhedral (E) or resorbed (R), while the blue/red font color highlights the eruptive style. For the pumices, the crystals were analyzed in crystal-separate mounts, while for lava flows in thin section. For the pumices, the crystal textures were evaluated only where rim-glass contact was exposed in the mount. Note the presence of abundant gas inclusions associated with skeletal growth in the Post-caldera dome samples (6R). The yellow arrows indicate the crystal-melt interface. The contact is used to evaluate whether crystals are resorbed or euhedral.

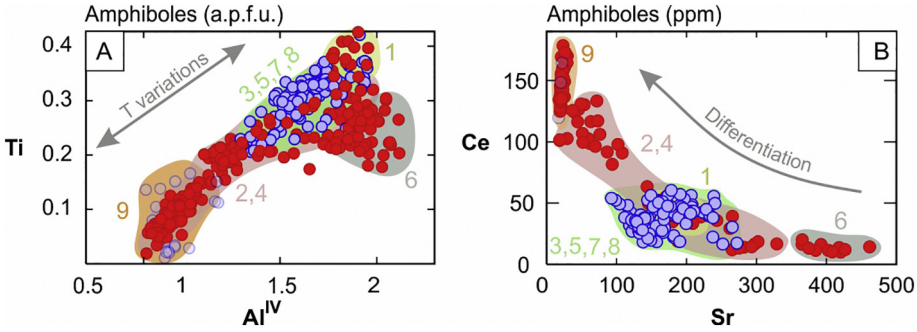

Fig. 7: EPMA (A) and LA-ICPMS (B) amphibole data (red – effusive; blue – explosive). The colored compositional fields are marked with numbers as in Figure 1. (A): The amphiboles from effusive units tend to evolve towards colder conditions, marked by the decrease in Al^{IV} and Ti. Units 1 and 6 are exceptions: 1 is older and hotter, while in 6 the amphibole compositions are biased by the less evolved chemical conditions of the system. (B): The LA-ICPMS trace element data shows the differentiation trend of amphiboles, where the REE-rich crystals correspond to the Al^{IV} and Ti poor samples from (A). Our data shows that the low Al amphibole crystals specific to upper-crustal silicic mushes, which were not identified in Klaver et al. (2017) are indeed present at Nisyros-Yali. Moreover, they indicate a progressive evolution from the hotter, high Al and high Ti populations.

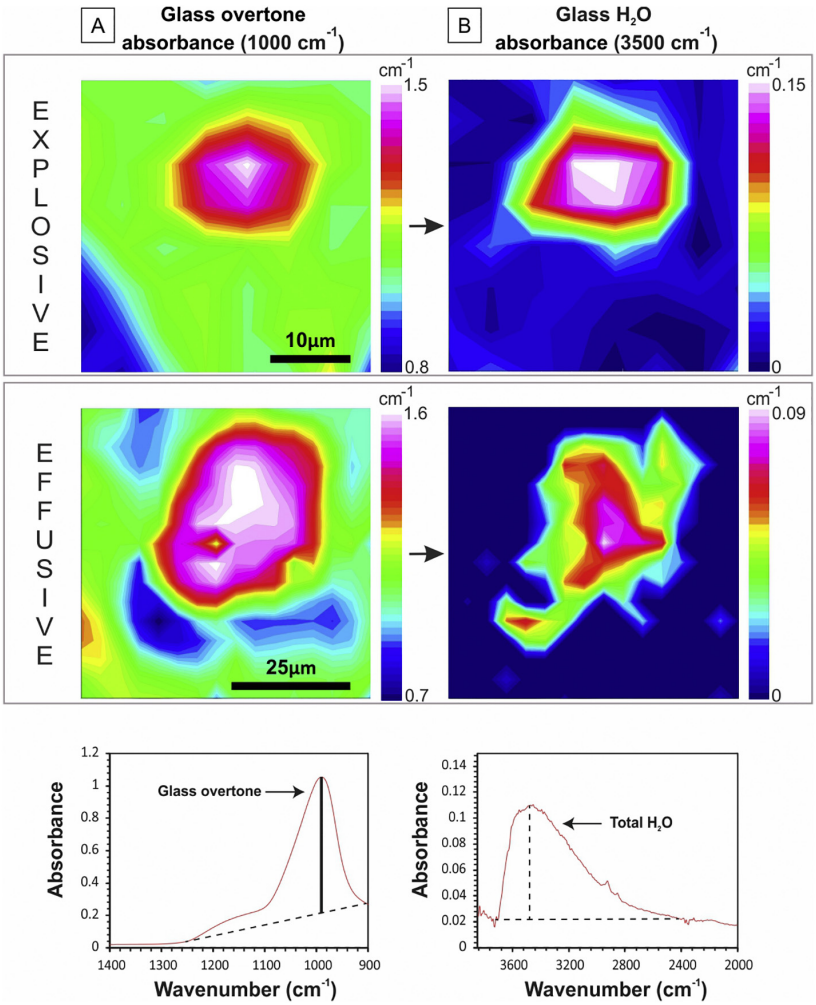

Fig. 8: An FTIR ATR+FPA overview of a typical melt inclusion from an explosive and effusive deposit. The two examples showcased are hosted by plagioclase crystals from the Upper Pumice and Avlaki lava flow. The shape and structural integrity of the melt inclusions can be seen in column (A): the absorbance maps of the glass overtone bands of the spectra. The water distribution inside the inclusions is shown in column (B): the absorbance maps of the total-water bands of the spectra. Note how water is distributed homogeneously in the melt inclusions preserved in fast-quenched pumices (first row). The opposite is seen in melt inclusions preserved in lava flows (second row): the non-homogeneous water distribution indicates water loss, possibly via post-emplacement diffusion. The lower diagrams indicate the bands of the spectra that were used to generate the Glass overtone and Total H_2O maps, respectively.

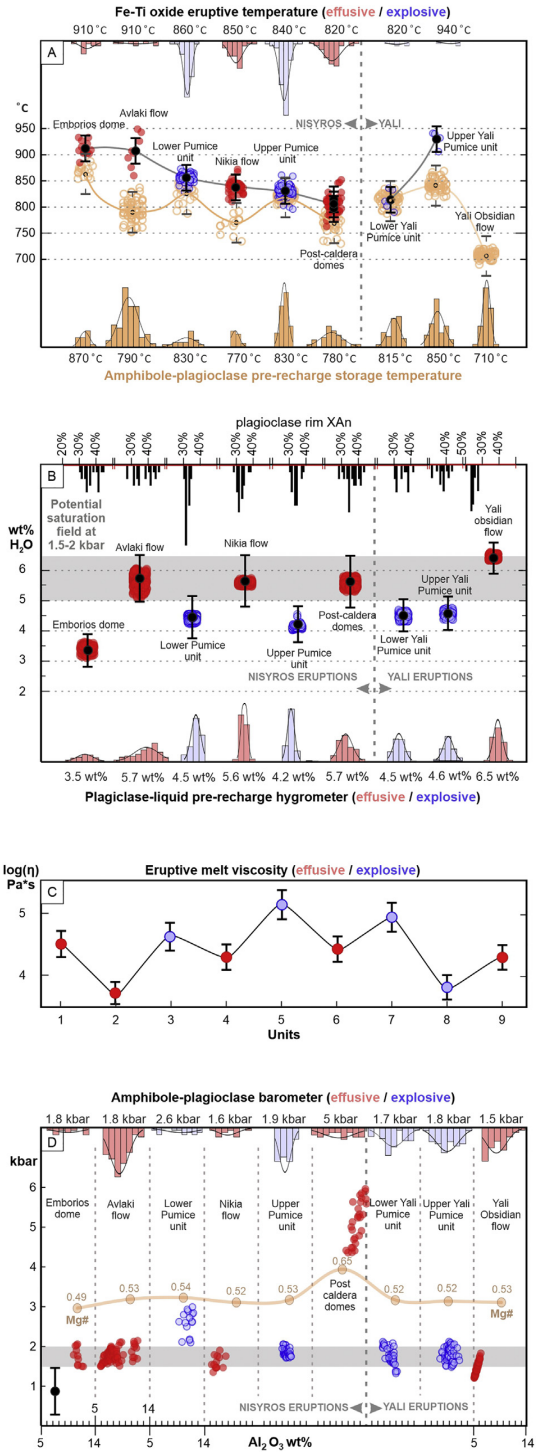

Fig. 9: Overview of storage and eruption conditions of Nisyros-Yali magmas. (A): Eruptive (red effusive, blue explosive) and pre-recharge storage temperatures (orange) derived from Fe-Ti oxide thermometry (±25˚C) (Ghiorso and Evans, 2008) and amphibole-plagioclase

thermometry (±40˚C), respectively (Holland and Blundy, 1994). The histograms indicate the statistical distribution of the data clouds. Note the larger ΔT corresponding to the effusive eruptions. (B): Water content estimated by plagioclase-liquid hygrometry (Waters and Lange, 2015) based on plagioclase rim – groundmass glass equilibria (Putirka, 2008). The upper histograms show the molar XAn% range used in the calculations. The lower histograms show the statistical distribution of the results. Error bars are standard hygrometer errors (±0.35 wt%) plus the propagated error given by the standard deviation of the storage temperature dataset. The cumulated hygrometry errors are less than ±0.7 wt% H_2O, but the statistical distribution of the dataset points at deviations of less than ±0.5 wt% from the average values of each unit (C) Calculated eruptive melt viscosity (±5% relative standard viscosity model error) (Giordano et al., 2008), using average groundmass-glass compositions, average eruptive temperatures (Fe-Ti oxide thermometry) and average water contents. In the case of the Yali Obsidian, an eruption temperature estimate is not available, so the temperature of the Yali Lower Pumice was used as input. (D) Storage pressure estimates (±0.6 kbar standard barometer error) based on plagioclase-amphibole barometry (Anderson and Smith, 1995). The x-axis shows the Al_2O_3 contents of the amphiboles used in the estimate. The orange curve gives the average Mg# of the amphibole populations. A correlation between Al_2O_3 and Mg# indicates a change in melt composition rather than a change in storage pressure. The upper histograms give the statistical distribution of the data.

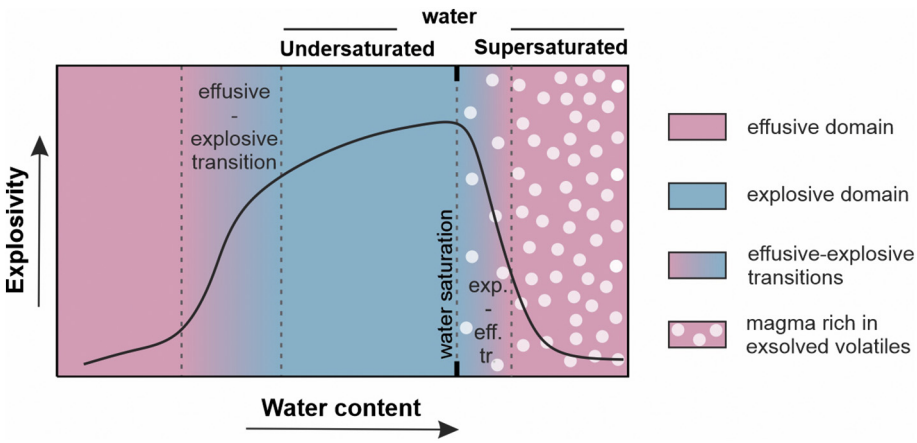

Fig. 10: Conceptual cartoon highlighting the effusive-explosive transition fields indicated by the Nisyros-Yali dataset. Increasing dissolved water contents favor the transition from effusive to explosive behavior until gas starts exsolving. In the supersaturated field, the transition to effusive eruptions is favored once more.

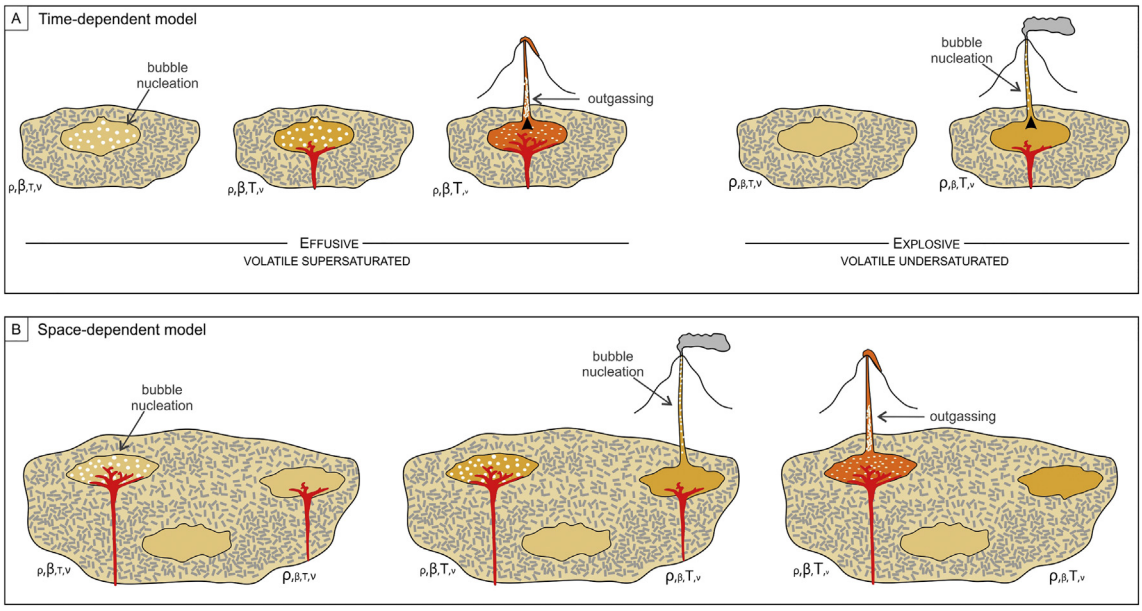

Fig. 11: Hypothesized - (A) Time-dependent and (B) Space-dependent models for effusive-explosive transitions at Nisyros-Yali, designed around the gas undersaturated and supersaturated states of the magma. The presence of a gas phase increases the bulk compressibility (β) and decreases the bulk density (ρ) of the magma reservoir. A hot recharge increases the temperature (T) of the magma as a factor of recharge melt fraction and mixing timescales, both dependent on compressibility (β). Viscosity (ν) is reduced as a consequence.

In the effusive scenario, gas bubbles are already available in the magma reservoir; therefore, permeability and outgassing develop early in the conduit. The Time-dependent model considers that the same eruptible area of the mush is responsible for triggering all eruptions. Alternatively, all eruptible areas share the same properties at the same moment in time. Longer residence-times, sufficient for advanced fractionation and volatile supersaturation are associated to effusive eruptions. The Space-dependent model considers a non-homogenous mush system with gas supersaturated and undersaturated pockets of melt coexisting in the same time frame. Here, the effusive-explosive transition is a function of which melt-pocket is tapped by the recharge melts. A combination of the two models is another plausible scenario.